

# FiLo++: Zero-/Few-Shot Anomaly Detection by Fused Fine-Grained Descriptions and Deformable Localization

Zhaopeng Gu, Bingke Zhu, Guibo Zhu, Yingying Chen, Ming Tang, *Member, IEEE*, Jinqiao Wang, *Member, IEEE*

**Abstract**—Anomaly detection methods typically require extensive normal samples from the target class for training, limiting their applicability in scenarios that require rapid adaptation, such as cold start. Zero-shot and few-shot anomaly detection do not require labeled samples from the target class in advance, making them a promising research direction. Existing zero-shot and few-shot approaches often leverage powerful multimodal models to detect and localize anomalies by comparing image-text similarity. However, their handcrafted generic descriptions fail to capture the diverse range of anomalies that may emerge in different objects, and simple patch-level image-text matching often struggles to localize anomalous regions of varying shapes and sizes. To address these issues, this paper proposes the FiLo++ method, which consists of two key components. The first component, Fused Fine-Grained Descriptions (FusDes), utilizes large language models to generate anomaly descriptions for each object category, combines both fixed and learnable prompt templates and applies a runtime prompt filtering method, producing more accurate and task-specific textual descriptions. The second component, Deformable Localization (DefLoc), integrates the vision foundation model Grounding DINO with position-enhanced text descriptions and a Multi-scale Deformable Cross-modal Interaction (MDCI) module, enabling accurate localization of anomalies with various shapes and sizes. In addition, we design a position-enhanced patch matching approach to improve few-shot anomaly detection performance. Experiments on multiple datasets demonstrate that FiLo++ achieves significant performance improvements compared with existing methods. Code will be available at <https://github.com/CASIA-IVA-Lab/FiLo>.

**Index Terms**—Anomaly detection, zero-shot learning, few-shot learning, multimodal learning.

## I. INTRODUCTION

**A**NOMALY detection is a highly practical task that finds wide application across diverse fields, including detecting product defects in industrial manufacturing [1]–[4],

Zhaopeng Gu and Ming Tang are with the Foundation Model Research Center, Institute of Automation, Chinese Academy of Sciences, Beijing 100190, China, and also with the School of Artificial Intelligence, University of Chinese Academy of Sciences, Beijing 100049, China (e-mail: guzhaopeng2023@ia.ac.cn; tangm@nlpr.ia.ac.cn).

Bingke Zhu and Yingying Chen are with the Foundation Model Research Center, Institute of Automation, Chinese Academy of Sciences, Beijing 100190, China, and also with the Objecteye Inc., Beijing 100190, China (email: bingke.zhu@nlpr.ia.ac.cn; yingying.chen@nlpr.ia.ac.cn).

Guibo Zhu is with the Foundation Model Research Center, Institute of Automation, Chinese Academy of Sciences, Beijing 100190, China, also with the School of Artificial Intelligence, University of Chinese Academy of Sciences, Beijing 100049, China, and also with the Shanghai Artificial Intelligence Laboratory, Shanghai 200232, China (e-mail: gbzhu@nlpr.ia.ac.cn).

Jinqiao Wang is with the Foundation Model Research Center, Institute of Automation, Chinese Academy of Sciences, Beijing 100190, China, also with the School of Artificial Intelligence, University of Chinese Academy of Sciences, Beijing 100049, China, also with the Wuhan AI Research, Wuhan 430073, China, and also with the Peng Cheng Laboratory, Shenzhen 518066, China (e-mail: jqwang@nlpr.ia.ac.cn).

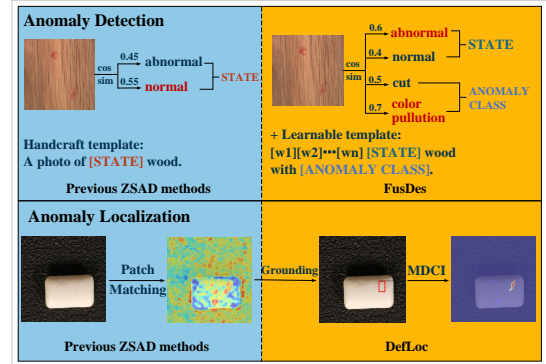


Fig. 1. Comparison of anomaly detection and localization between FiLo++ and previous ZSAD methods. Previous ZSAD methods utilize generic anomaly descriptions, which may lead to errors. Our FusDes enhances detection accuracy by fine-grained anomaly descriptions, learnable templates, and runtime prompt filtering. For localization, existing ZSAD methods typically compare image patches directly with text features, resulting in false positives in background regions. Our DefLoc method effectively eliminates background areas and improves localization accuracy by employing Grounding DINO, position-enhanced text descriptions, and the MDCI module.

identifying lesions in medical contexts [5], [6], and monitoring abnormal behaviors of vehicles and pedestrians in transportation [7]–[9]. Traditional anomaly detection methods [10]–[12] typically regard the problem as one-class classification, where the model is trained on a large number of normal samples and subsequently attempts to detect out-of-distribution anomalies. Although these methods perform well, they lose effectiveness in scenarios where large-scale normal data collection is challenging (e.g., cold-start settings). Consequently, zero-shot and few-shot anomaly detection methods [13]–[15], which do not require prior data from the target category, have gained considerable attention. In these methods, only a small number of normal samples are optionally provided as references during testing, and the methods can detect object categories that have never been encountered during training.

Existing zero-shot and few-shot anomaly detection approaches [13]–[15] primarily build on multimodal pre-trained models such as CLIP [16]. Trained on extremely large-scale image-text pair datasets, multimodal models exhibit remarkable zero-shot performance in image classification [17], semantic segmentation [18], [19], and object detection [20]. Anomaly detection methods based on multimodal pretrained models [13], [15] often rely on handcrafted text prompts conveying “normal” and “abnormal” semantics, then determine whether each image patch is anomalous by comparing its feature similarity to text embeddings. Such techniques offer a solution for both Zero-Shot Anomaly Detection (ZSAD)

and Few-Shot Anomaly Detection (FSAD), yet they face limitations in two main aspects. First, regarding detection, manually crafted general descriptions lack flexibility and fail to capture the diverse types of anomalies across different object categories. Second, for localization, naively matching patch features with text prompts struggles to detect anomalous regions that span multiple patches or have varying shapes.

In response to these challenges, this paper proposes a method called FiLo++, which offers effective solutions for anomaly detection and localization. For detection, we design a **Fused Fine-Grained Descriptions** (FusDes) module to improve anomaly detection. First, this module leverages the extensive cross-domain knowledge of Large Language Models (LLMs) to generate specific types of anomalies potentially appearing in the test sample, replacing the generic, manually crafted prompts with content more tailored to each test sample. Second, existing research shows that the template of the text prompt in multimodal models significantly affects performance. Prior methods usually adopt the prompt template from CLIP [16] that is originally designed for ImageNet classification [21], which may not fully suit anomaly detection tasks. To this end, we introduce new prompt templates specialized for anomaly detection and combine fixed, human-designed templates with learnable, adaptive templates to produce text prompts better suited to anomaly detection. Finally, we propose a runtime prompt filtering strategy that boosts the distinguishability between normal and abnormal text features, yielding the final fused fine-grained description. Compared to the “normal” vs. “abnormal” general descriptions used by existing methods, the FusDes module, which combines LLM priors, fixed and learnable prompt templates and runtime filtering, substantially enhances anomaly detection capabilities.

For localization, we design a **Deformable Localization** (DefLoc) module to overcome difficulties in localizing anomalous regions of various sizes and shapes across multiple patches. This module proceeds in three main steps. First, DefLoc utilizes detailed anomaly information generated by the LLMs and employs the vision foundation model Grounding DINO [20] for initial anomaly localization. Although Grounding DINO alone shows poor performance in anomaly detection, it effectively filters out backgrounds and homogeneous areas irrelevant to anomalies, thus helping subsequent localization steps. Second, DefLoc integrates the positional information from Grounding DINO’s initial localization results into the text descriptions, making them more accurate. Third, DefLoc applies a Multi-scale Deformable Cross-modal Interaction (MDCI) module, which aggregates image patch features using deformable convolutions [22] at multiple scales and thereby strengthens detection of anomalous regions with different shapes and sizes.

Furthermore, we design a position-enhanced patch matching approach to support few-shot anomaly detection. By leveraging the preliminary localization results from the DefLoc module, we constrain the scope of patch matching to improve detection and localization performance in FSAD scenarios.

FiLo++ is an extension of our work FiLo [15], which is published in ACM MM 2024. Compared to FiLo, FiLo++ makes three primary improvements: 1) FiLo++ replaces the

FG-Des module with the FusDes module that merges fixed prompt templates, learnable templates, and runtime prompt filtering to further enhance the alignment between text and image features.; 2) FiLo++ employs multi-scale deformable convolutions in place of standard convolutions in the DefLoc module to better detect anomalies of different shapes and sizes; 3) FiLo++ adds a FSAD branch that utilizes DefLoc’s initial localization results to refine patch matching, expanding the applicability of the FiLo++. Beyond making structural modifications, we further conduct experiments under various settings and carry out more extensive ablation studies to provide a comprehensive evaluation of our method.

We perform extensive experiments on various datasets such as MVTec-AD [23] and VisA [24], and results show that FiLo++ achieves significant improvements in ZSAD and FSAD. For instance, in the zero-shot scenario on VisA, FiLo++ achieves an image-level AUC of 84.5% and a pixel-level AUC of 96.2%.

Our contributions can be summarized as follows:

- We propose a FusDes approach that leverages cross-domain knowledge in LLMs to generate detailed anomaly descriptions. By combining fixed text prompt templates with learnable templates and applying a runtime prompt filtering method, we produce text features more suitable for anomaly detection, thereby enhancing both accuracy and interpretability.
- Additionally, we introduce a DefLoc module that integrates preliminary anomaly localization from the Grounding DINO vision foundation model, position-enhanced text descriptions, and a Multi-scale Deformable Cross-modal Interaction (MDCI) module to more accurately localize anomalies of different sizes and shapes. Furthermore, by incorporating a few-shot anomaly detection branch, FiLo++ can perform both ZSAD and FSAD, improving its flexibility and generalization.
- Extensive experiments on multiple datasets show that FiLo++ significantly outperforms baseline methods. Experimental results prove effective for both zero-shot and few-shot anomaly detection and localization, achieving state-of-the-art performance.

## II. RELATED WORK

### A. Zero-shot Anomaly Detection

Following the remarkable success of the multimodal pre-trained CLIP [16] in various zero-shot settings within computer vision, numerous studies now leverage CLIP’s powerful capabilities to conduct zero-shot anomaly detection. Early explorations such as CLIP-AD [25] and ZoC [26] directly apply CLIP to anomaly detection datasets by comparing overall image features with textual descriptors such as “normal” and “abnormal.” However, these methods exhibit relatively poor performance and cannot localize anomalies. WinCLIP [13] is the first CLIP-based anomaly detection method that enables anomaly localization by sliding windows of various sizes across an image and determining anomalous regions through each window’s anomaly score. Although WinCLIP achieves preliminary anomaly localization, it introduces substantial

computational overhead. APRIL-GAN [27] mitigates WinCLIP’s excessive computation by training an additional linear layer to align text features with patch-level image features. CLIP Surgery [28] then first introduces V-V Attention to naturally align patch-level image features and text features, and AnoVL [29] extends this approach with anomaly-specific text templates and runtime adapters to enhance detection results. AnomalyCLIP [30] replaces handcrafted text with an object-agnostic learnable text vector but only employs the single word “damaged” for all anomalies, failing to capture richer anomaly categories. In contrast, FiLo++ employs LLMs to generate detailed anomaly categories, combines handcrafted templates with learnable text vectors, and introduces a runtime prompt filtering strategy to obtain text features better suited for anomaly detection, enhancing detection accuracy.

Regarding anomaly localization, Segment Any Anomaly (SAA) [31] represents a line of work that uses foundational vision models such as Grounding DINO [20] and the Segment Anything Model [32] to segment anomalous regions. However, two main issues arise: first, these methods only segment anomalies when they confirm that an object contains anomalies and thus cannot ascertain whether anomalies exist in the first place; second, SAA’s segmentation heavily depends on Grounding DINO. Because there is a considerable distribution shift between anomaly detection data and Grounding DINO’s pretraining data, direct application of Grounding DINO yields low accuracy, numerous false positives, or labels an entire object as anomalous. Nevertheless, Grounding DINO excels at detecting foreground objects and efficiently filters out background or uniformly normal regions. Therefore, in FiLo++’s DefLoc module, we only employ Grounding DINO for preliminary anomaly localization to improve the performance of subsequent localization steps.

### B. Few-shot Anomaly Detection

Compared with zero-shot anomaly detection, few-shot anomaly detection allows a model to access a small number of normal reference samples from the same category as the test data. Patch-level feature comparison [1], [10], [14] is the most prevalent approach here: these methods detect anomalies by comparing patch-level features from the test sample with those from the normal sample. Building on this vanilla patch feature matching, some works propose various improvements. For example, RegAD [14] adopts STN [33] for image registration to improve matching precision, ADformer [1] employs a CNN-Transformer composite architecture to extract more effective features, and COFT-AD [34] uses contrastive learning to fine-tune the feature extractor. In FiLo++, we utilize the preliminary anomaly localization result from the DefLoc module to constrain the regions involved in patch feature matching and then integrate the results of patch-level matching with image-text feature matching to further enhance FSAD performance.

### C. Multi-Scale Convolution

Multi-scale convolution combines convolution kernels of different receptive field sizes, enabling effective feature extraction for objects of various sizes in an image. This approach

has demonstrated outstanding performance in numerous vision tasks and has become highly popular in computer vision research. InceptionNet [35] is a pioneering example that uses  $1\times 1$ ,  $3\times 3$ , and  $5\times 5$  kernels in parallel within the same layer and then concatenates the results along the channel dimension. RepVGG [36] decomposes larger convolution kernels into multiple  $3\times 3$  kernels, substantially reducing model parameters and improving inference speed. MixConv [37] applies different kernel sizes to different channels within the same convolution operation, balancing multi-scale benefits and computational efficiency. Nevertheless, these methods all rely on fixed-shaped kernels, which lack flexibility. Deformable Convolution Network [22] introduces deformable convolution operations that greatly enhance feature extraction for objects with irregular shapes, which is highly beneficial for anomaly detection. In FiLo++, we incorporate both multi-scale and deformable convolutions, fully leveraging multimodal image-text features to design the MDCI module, which accurately localizes anomalies of various sizes and shapes.

## III. METHOD

### A. Overview

This paper proposes a novel zero-shot and few-shot anomaly detection method, FiLo++, which enhances the performance of anomaly detection and localization through two modules: FusDes and DefLoc. Specifically, for anomaly detection, we design the Fused Fine-Grained Description module (FusDes, Section III-B), which leverages detailed anomaly descriptions provided by large language models. FusDes combines fixed templates with learnable text vectors and implements a runtime prompt filtering strategy to obtain text features that more accurately match anomaly detection images. The FusDes module not only determines whether an image contains anomalies but also identifies the specific types of anomalies within the image, significantly improving the interpretability of the method. For anomaly localization, we develop the Deformable Localization module (DefLoc, Section III-C), which accurately locates anomalies of varying sizes and dimensions through initial localization using Grounding DINO, position-enhanced text descriptions, and a Multi-scale Deformable Cross-modal Interaction module.

### B. FusDes

Numerous existing methods demonstrate that the quality of text prompts significantly affects the performance of anomaly detection based on image-text pre-trained models when inferring new categories. Therefore, we first investigate prompt engineering to generate more precise and efficient text prompts to enhance detection accuracy. The FusDes module consists of three main components: 1) generation of fine-grained anomaly descriptions based on LLMs; 2) combination of fixed templates with learnable text vectors; and 3) runtime prompt filtering. These three components are detailed below.

1) *Fine-Grained Anomaly Descriptions*: Initial CLIP-based anomaly detection methods use terms like “abnormal” to represent anomaly semantics, which fail to capture the diversity of anomaly types. WinCLIP expands anomaly description

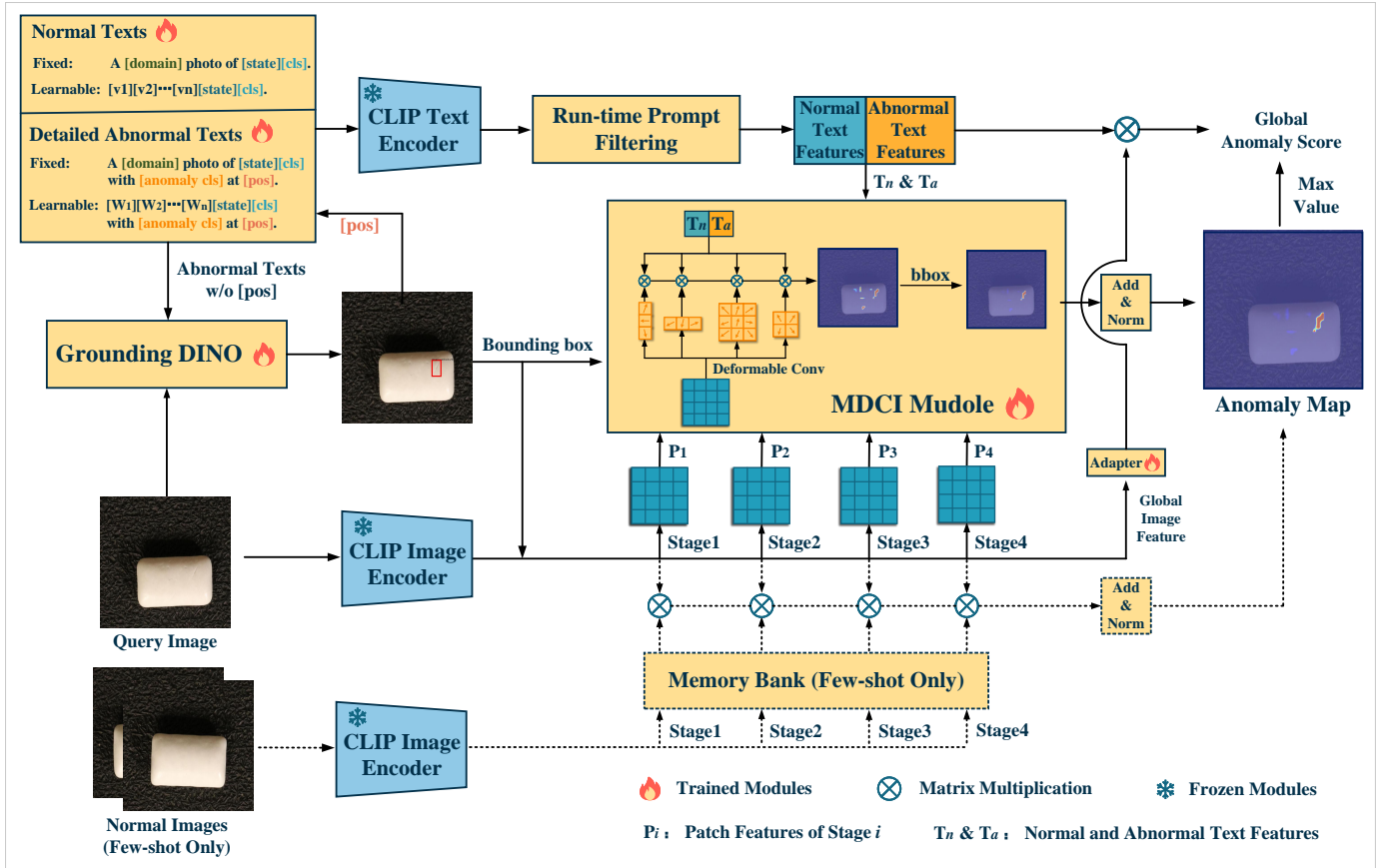


Fig. 2. Overall architecture of FiLo++. Given an input image, an LLM generates fine-grained anomaly types. The normal and detailed anomaly texts are processed by Grounding DINO to obtain bounding boxes, then combined with fixed and learnable templates and encoded by the CLIP Text Encoder with runtime prompt filtering to produce  $T_n$  and  $T_a$ . The image’s intermediate patch features interact with the text features through the MDCI module to create the vision-language anomaly map. A few-shot anomaly map is generated using the memory bank of few-shot normal samples. Finally, global image features are compared with the fused text features to obtain the global anomaly score.

texts by including terms such as “damaged,” “flaw,” and “defect.” However, these descriptions remain broad and cannot accurately describe different anomaly types on various objects. We require more specific and precise anomaly descriptions to match the rich variety of anomalies. Large language models (LLMs), such as GPT-4, trained on vast image and text datasets, possess extensive “world knowledge” across various domains. We utilize the powerful knowledge of LLMs to generate detailed anomaly types for each test sample, resulting in more accurate fine-grained descriptions than generic terms like “damaged” or “abnormal.” These detailed descriptions better match the test images, improving detection precision and enabling the determination of specific anomaly contents in the images based on the similarity between text descriptions and image content, thereby enhancing the method’s interpretability.

2) *Combination of Fixed Templates and Learnable Text Vectors*: After methods like WinCLIP achieve excellent performance on multiple anomaly detection datasets, subsequent approaches typically adopt the same text templates used by WinCLIP to construct text prompts. However, the text template *A photo of [class]*, used in WinCLIP is primarily derived from templates employed by CLIP for image classification tasks on the ImageNet dataset, which focus on indicating the foreground object category rather than whether the object

contains anomalous parts. Therefore, we modify this template by incorporating the fine-grained descriptions generated by LLMs, changing it to *A [domain] photo of [state] [cls] (with [anomaly cls] at [pos])*. Here, *[domain]* represents the object’s domain, *[state]* indicates normal or anomalous status, and *[cls]* denotes the object category name. For anomaly descriptions, the template includes *[anomaly cls]* for detailed anomaly content and *[pos]* for anomaly location, categorized into nine positions: top-left, left, bottom-left, top, center, bottom, top-right, right, and bottom-right.

The modified template significantly enhances both performance and interpretability compared to the original. However, manually crafted templates cannot achieve the optimal solution for anomaly detection tasks. Consequently, we introduce learnable adaptive text templates trained with relevant anomaly detection data. These templates adaptively learn text prompts that better distinguish between normal and anomalous samples based on the image’s normal and anomalous content. The adaptive normal and anomalous text templates are defined as follows:

$$T_n = [V_1][V_2] \dots [V_n][state][cls]$$

$$T_a = [W_1][W_2] \dots [W_n][state][cls]$$

*with [anomaly cls] at [pos]*

where  $[V_i]$  and  $[W_i]$  are learnable text vectors, and  $T_n$  and  $T_a$  represent the normal and anomalous text templates.

By inserting the fine-grained anomaly descriptions generated by LLMs into the *[anomaly cls]* field of the adaptive text templates, we obtain complete text prompts. These fine-grained anomaly descriptions not only enhance detection accuracy but also improve the interpretability of the detection results. Specifically, we calculate the similarity between image features and each detailed anomaly description’s text features. By examining the content of text descriptions with high similarity, we determine the specific anomaly category within the image, thereby gaining a deeper understanding of the model’s decision-making process.

3) *Runtime Prompt Filtering*: Ideally, anomaly detection methods based on image-text multimodal models should associate normal images with normal texts and anomalous images with anomalous texts, such that the similarity between normal image features and normal text features exceeds that between normal images and anomalous texts, and vice versa. However, in practice, we observe overlapping distances between normal and anomalous text features, a phenomenon termed cross-semantic ambiguity [38], which hinders anomaly detection. Specifically, for the set of normal text features  $T_n^{origin} = \{T_{n,1}, T_{n,2}, \dots\}$  and anomalous text features  $T_a^{origin} = \{T_{a,1}, T_{a,2}, \dots\}$ , we first compute the cosine distances between the test image features and each feature in both sets, resulting in distance sets  $D_n = \{D_{n,1}, D_{n,2}, \dots\}$  and  $D_a = \{D_{a,1}, D_{a,2}, \dots\}$ . Ideally, for an image, the distance sets  $D_n$  and  $D_a$  should be mutually exclusive or have minimal overlap, meaning that for normal images,  $D_n$  should be significantly smaller than  $D_a$ , and for anomalous images,  $D_a$  should be significantly smaller than  $D_n$ . However, due to the diversity of text descriptions, not all text descriptions are reflected in a single test image, resulting in some noisy descriptions that may negatively impact model performance.

To address this issue, we design a strategy to filter the overlapping prompts in  $D_n$  and  $D_a$ . Specifically, we first determine the overlapping interval as follows:

$$D_c = [\max(\min(D_n), \min(D_a)), \min(\max(D_n), \max(D_a))].$$

We then remove the prompts in  $D_n$  and  $D_a$  that fall within  $D_c$ , thereby completing runtime prompt filtering and obtaining the filtered text feature sets  $T_n$  and  $T_a$ .

Next, we compute the global anomaly score by calculating the similarity between the global image feature  $G$ , obtained by passing the image through the CLIP image encoder and adapter, and the filtered text features  $T_n$  and  $T_a$ :

$$S_{global} = \text{softmax}(G \cdot [T_n, T_a]^T) + \max(M), \quad (1)$$

where  $M$  denotes the anomaly map calculated in Section III-C, and  $\max(\cdot)$  represents the maximum operation. The adapter has a bottleneck structure to align global image features and text features, consisting of two linear layers, one ReLU [39] layer, and one SiLU [40] layer, as shown in Algorithm 1.

The FusDes module not only improves anomaly detection accuracy but also enhances the interpretability of the detection results. By evaluating the similarity between image features

---

### Algorithm 1 Adapter Module

---

**Input:** vector  $\mathbf{x}$

**Output:** vector  $\mathbf{y}$

- 1:  $\mathbf{h}_1 = \text{ReLU}(\mathbf{W}_1\mathbf{x} + \mathbf{b}_1)$
  - 2:  $\mathbf{y} = \text{SiLU}(\mathbf{W}_2\mathbf{h}_1 + \mathbf{b}_2)$
- 

and each detailed description’s text features, we can identify the text descriptions that best match the image, thereby determining the specific anomaly types present in the image.

### C. DefLoc

Existing anomaly detection methods locate anomalous patches by directly computing the similarity between each image patch’s features and text features. However, an anomalous region often spans multiple patches, and different anomalous regions vary in position, shape, and size. Sometimes, it is necessary to consider the surrounding normal regions to determine whether a region is anomalous. To address these challenges, we design the DefLoc module, which utilizes initial localization via Grounding DINO, position-enhanced text prompts, and a Multi-scale Deformable Cross-modal Interaction (MDCI) module to accurately locate anomalous regions of varying sizes and shapes. Additionally, we introduce a few-shot anomaly detection branch that employs a position-enhanced patch matching approach to achieve more accurate few-shot anomaly detection and localization results.

1) *Initial Localization with Grounding DINO*: Previous multimodal pre-trained model-based anomaly detection methods typically treat patches from different image locations equally when computing similarity with text features. However, the object under inspection often occupies only a portion of the input image, with the remaining background requiring exclusion. Direct patch similarity computation may erroneously identify minor disturbances in the background as anomalous regions, leading to false detections. We utilize the detailed anomaly descriptions generated by FusDes and employ the Grounding DINO method for initial anomaly localization. Although Grounding DINO alone cannot precisely determine the exact anomaly locations, the resulting bounding boxes generally encompass the foreground objects. Therefore, we use Grounding DINO’s localization results to restrict the anomaly regions, effectively avoiding false detections in the background and improving the accuracy of subsequent anomaly localization. Furthermore, since Grounding DINO may occasionally miss some anomalies, we do not adopt an all-or-nothing approach for regions outside the bounding boxes. Instead, we suppress the anomaly scores of regions outside all Grounding DINO bounding boxes by multiplying them by a hyperparameter  $\lambda$ , thereby mitigating potential misses caused by Grounding DINO.

2) *Position-Enhanced Text Prompts*: After obtaining initial anomaly localization results with Grounding DINO, we incorporate the positional information of the bounding boxes into the text prompts to enhance position descriptions. Specifically, we categorize the anomaly positions within the image into nine regions: top-left, left, bottom-left, top, center, bottom,

top-right, right, and bottom-right. Based on the center coordinates of the Grounding DINO bounding boxes, we determine which positions are likely to contain anomalies and add this positional information to the  $[pos]$  field of the text prompts. Text prompts enriched with detailed anomaly descriptions and positional information better match the content of the image under inspection, facilitating the model to focus on specific regions during subsequent anomaly localization and thereby improving localization precision.

3) *Multi-scale Deformable Cross-modal Interaction*: To accurately localize anomalous regions of different shapes and sizes, our method does not directly compute the similarity between each image patch feature and text features. Instead, we design a Multi-scale Deformable Cross-modal Interaction (MDCI) module. The design of MDCI is inspired by WinCLIP’s approach of selecting image subregions using sliding windows of different sizes, but it overcomes the computational overhead of inputting dozens of differently sized images into the Image Encoder simultaneously as in WinCLIP. Specifically, we design deformable convolution kernels of varying sizes and shapes to aggregate regions of the patch features extracted by the CLIP Image Encoder in parallel. We then compute the similarity between the aggregated features and the position-enhanced text features, performing text feature-guided multi-scale deformable convolution operations. This approach allows the MDCI module to handle anomalous regions of varying sizes and shapes simultaneously, significantly enhancing the model’s ability to localize anomalies while maintaining high computational efficiency.

Specifically, we design  $n$  deformable convolution kernels of different sizes and shapes, denoted as  $D_j$ , where  $j$  ranges from 1 to  $n$ . For each stage  $i$ , the patch features  $P_i \in \mathbb{R}^{H_i W_i \times C}$  extracted by image encoder, along with the position-enhanced text features  $[T_n, T_a] \in \mathbb{R}^{2 \times C}$ , are processed as follows:

$$M_i^n, M_i^a = \text{Up}(\text{Norm}(\sum_{j=1}^n S(D_j(P_i) \cdot [T_n, T_a]^T))), \quad (2)$$

where  $\text{Up}(\cdot)$  denotes upsampling,  $S(\cdot)$  represents the Softmax operation, and  $\text{Norm}(\cdot)$  denotes the normalization operation. By summing and normalizing the maps from each stage, we obtain the final normal and anomaly maps:

$$M^n = \text{Norm}\left(\sum_i M_i^n\right), \quad M^a = \text{Norm}\left(\sum_i M_i^a\right). \quad (3)$$

The anomaly localization result obtained through this vision-language feature comparison method is expressed as:

$$M^{vl} = \frac{M^a + (1 - M^n)}{2}. \quad (4)$$

4) *Few-shot Anomaly Detection Branch*: In the newly added few-shot anomaly detection branch, we design a position-enhanced patch matching method that utilizes the initial localization information obtained from DefLoc to constrain the patch matching regions. Specifically, in the few-shot anomaly detection branch, we first use the same CLIP image encoder to extract patch-level features from known normal image samples and store each stage’s features in the

corresponding memory bank. Then, for each stage  $i$  of the query image’s patch features  $P_i$ , we calculate the cosine distance between  $P_i$  and all normal patch features in the corresponding memory bank, selecting the minimum cosine distance as the anomaly score for that patch at that stage:

$$M_i^{few} = \min(\text{cos\_distance}(P_i, \text{Mem}_i)), \quad (5)$$

where  $\text{Mem}_i$  represents the memory bank for stage  $i$ . By summing and normalizing the anomaly scores across all stages and suppressing the scores of regions outside the Grounding DINO bounding boxes, we obtain the few-shot anomaly localization result:

$$M^{few} = \text{Norm}\left(\sum_i M_i^{few}\right). \quad (6)$$

Combining the few-shot anomaly localization results with the image-text anomaly localization results, we obtain the final anomaly localization result:

$$M = G_\sigma\left(\frac{M^{vl} + M^{few}}{2}\right), \quad (7)$$

where  $G_\sigma$  is a Gaussian filter, and  $\sigma$  is a hyperparameter controlling the degree of smoothing, set to 4 in our experiments.

#### D. Loss Functions

To learn the content of adaptive text templates and the parameters in MDCI and adapter, we choose different loss functions for training from the perspectives of global anomaly detection and local anomaly localization. We choose the cross-entropy loss as our global loss for global anomaly detection, as it is a commonly used binary classification loss function. The global loss is computed as follows:

$$L_{global} = L_{ce}(S_{global}, Label), \quad (8)$$

where  $S_{global}$  is the global anomaly score computed in Sec. III-B, and  $Label$  indicates whether the image is anomalous or not. For local anomaly localization, we employ Focal loss [41] and Dice loss [42] to optimize the anomaly map. Both losses are commonly used in semantic segmentation. Focal loss leverages the parameter  $\gamma$  to increase the weighting of hard examples, thereby addressing class imbalance, while Dice loss optimizes segmentation quality based on the Dice coefficient. Our local loss is calculated as:

$$L_{local} = L_f(M^a, G) + L_d(M^a, G) + L_d(M^n, 1 - G), \quad (9)$$

where  $G$  denotes the ground truth.

## IV. EXPERIMENTS

### A. Datasets

We conduct experiments primarily on the MVTEC-AD [23] and VisA [24] datasets. MVTEC-AD is a comprehensive industrial anomaly detection dataset, comprising 5,354 images from 15 different categories, including 10 object categories and 5 texture categories, with resolutions ranging from  $700 \times 700$  to  $1,024 \times 1,024$  pixels. In comparison, the VisA dataset presents

TABLE I

COMPARISON RESULTS BETWEEN FiLo++ AND OTHER ZSAD METHODS. *Img-AUC* AND *Px-AUC* IN TABLE REPRESENT IMAGE-LEVEL AUC AND PIXEL-LEVEL AUC. THE BEST-PERFORMING METHOD IS IN **BOLD**.

Method	MVTec-AD		VisA	
	Img-AUC	Px-AUC	Img-AUC	Px-AUC
CLIP [16]	74.1	38.4	66.4	46.6
CLIP-AC [16]	71.5	38.2	65.0	47.8
WinCLIP [13]	91.8	85.1	78.1	79.6
APRIL-GAN [27]	86.1	87.6	78.0	94.2
AnomalyCLIP [30]	91.5	91.1	82.1	95.5
FiLo [15]	91.2	92.3	83.9	95.9
<b>FiLo++ (ours)</b>	<b>92.1</b>	<b>92.8</b>	<b>84.5</b>	<b>96.2</b>

TABLE II

COMPARISON RESULTS BETWEEN FiLo++ AND OTHER FSAD METHODS. *Img-AUC* AND *Px-AUC* IN TABLE REPRESENT IMAGE-LEVEL AUC AND PIXEL-LEVEL AUC. THE BEST-PERFORMING METHOD IS IN **BOLD**.

Setup	Method	MVTec-AD		VisA	
		Img-AUC	Px-AUC	Img-AUC	Px-AUC
1-shot	SPADE	81.0	91.2	79.5	95.6
	PatchCore	83.4	92.0	79.9	95.4
	WinCLIP	93.1	95.2	83.8	96.4
	AnomalyGPT	94.1	95.3	87.4	96.2
	<b>FiLo++ (ours)</b>	<b>95.0</b>	<b>96.2</b>	<b>88.3</b>	<b>97.3</b>
2-shot	SPADE	82.9	92.0	80.7	96.2
	PatchCore	86.3	93.3	81.6	96.1
	WinCLIP	94.4	96.0	84.6	96.8
	AnomalyGPT	95.5	95.6	<b>88.6</b>	96.4
	<b>FiLo++ (ours)</b>	<b>95.8</b>	<b>96.5</b>	<b>88.6</b>	<b>97.5</b>
4-shot	SPADE	84.8	92.7	81.7	96.6
	PatchCore	88.8	94.3	85.3	96.8
	WinCLIP	95.2	96.2	87.3	97.2
	AnomalyGPT	<b>96.3</b>	96.2	<b>90.6</b>	96.7
	<b>FiLo++ (ours)</b>	<b>96.3</b>	<b>96.6</b>	89.8	<b>97.9</b>

greater challenges, containing 10,821 images from 12 different categories, with resolutions of 1, 500×1, 000 pixels. Consistent with APRIL-GAN [27] and AnomalyCLIP [30], we perform supervised training on one dataset and conduct zero-shot or few-shot testing on the other dataset.

### B. Evaluation Metrics

Consistent with existing zero-shot and few-shot anomaly detection methods [2], [12], [43], we employ the Area Under the Receiver Operating Characteristic (AUC) as the evaluation metric. Image-level AUC is utilized to assess the performance of anomaly detection, while pixel-level AUC evaluates the performance of anomaly localization.

### C. Implementation Details

We employ the publicly available CLIP-L/14@336px model as the backbone, freezing the parameters of both the CLIP text encoder and image encoder. Training is conducted on either the MVTec-AD or VisA dataset, while zero-shot and few-shot testing is performed on the other dataset. For intermediate layer patch features, we utilize the features from the 6th, 12th, 18th, and 24th layers of the CLIP image encoder. Starting

TABLE III

ABLATION RESULTS FOR ANOMALY DESCRIPTIONS. *GS* STANDS FOR GENERIC STATE, *FGD* FOR FINE-GRAINED DESCRIPTION, *LT* FOR LEARNABLE TEMPLATE, AND *RTPF* FOR RUNTIME PROMPT FILTERING. *Img-AUC* AND *Px-AUC* REPRESENT IMAGE-LEVEL AND PIXEL-LEVEL AUC, RESPECTIVELY. THE BEST-PERFORMING RESULT IS IN **BOLD**.

Setup	MVTec-AD		VisA	
	Img-AUC	Px-AUC	Img-AUC	Px-AUC
CLIP baseline	71.5	38.2	65.0	47.8
+ GS	79.9	83.5	65.4	83.9
+ FGD	80.8	83.8	71.2	85.5
+ LT	85.8	85.1	78.1	93.2
<b>+ RTPF</b>	<b>86.2</b>	<b>85.3</b>	<b>78.5</b>	<b>93.5</b>

from the 7th layer, we simultaneously leverage the outputs of QKV Attention and V-V Attention, where the output of QKV Attention is aligned with text features through a simple linear layer, and the output of V-V Attention is input into the MDCI module for multi-scale and multi-shape deep interaction with text features. During training, input images are resized to a resolution of 518 × 518 and the model parameters are optimized for 15 epochs using the AdamW optimizer [44]. The learning rate for the learnable text vectors is set to 1e-3, while the learning rate for the MDCI module is set to 1e-4. Subsequently, we train the adapter for 5 epochs with a learning rate of 1e-5. Additionally, due to the varying number of fine-grained anomaly descriptions across object categories, training is conducted with a batch size of 1. Following previous methods [12], [30], a Gaussian filter with  $\sigma = 4$  is applied during testing to obtain smoother anomaly score maps. We use the GPT-4o model in our paper and the prompt that we use is: “Based on your knowledge, what anomalies might occur on [class name]?”

### D. Zero-shot Results

To demonstrate the effectiveness of our proposed FiLo++, we compare it against several existing zero-shot anomaly detection methods, including CLIP [16], CLIP-AC [16], WinCLIP [13], APRIL-GAN [27], AnomalyCLIP [30] and FiLo [15]. Following the methodology of AnomalyCLIP [30], we conduct experiments with CLIP using straightforward text prompts such as “A photo of a normal [class].” and “A photo of an anomalous [class].” Additionally, for CLIP-AC, we incorporate a variety of text prompt templates recommended for the ImageNet dataset to enhance performance. The results for WinCLIP [13], APRIL-GAN [27], and AnomalyCLIP [30] are directly adopted from their respective publications.

Table I presents a performance comparison between FiLo++ and other zero-shot anomaly detection methods. The results indicate that FiLo++ outperforms existing ZSAD approaches in both anomaly detection and localization, thereby demonstrating the effectiveness of the FusDes and DefLoc modules we have designed.

### E. Few-shot Results

In order to further validate the effectiveness of FiLo++ in few-shot anomaly detection, we compared its perfor-

TABLE IV  
THE RESULTS OF ABLATION EXPERIMENTS FOR EACH PROPOSED MODULES IN DEFLOC. THE BEST-PERFORMING RESULT IS IN BOLD.

Grounding	Position Enhancement	MDCI			MVTec-AD		VisA	
		Multi-shape	Multi-scale	Deformable	Image-AUC	Pixel-AUC	Image-AUC	Pixel-AUC
					86.2	85.3	78.5	93.5
✓					86.2	85.7	78.5	93.9
✓	✓				86.5	85.9	78.6	94.1
✓	✓	✓			86.8	89.6	79.4	95.6
✓	✓		✓		89.3	91.7	81.2	95.9
✓	✓	✓	✓		91.4	92.3	84.1	95.9
✓	✓	✓	✓	✓	<b>92.1</b>	<b>92.8</b>	<b>84.5</b>	<b>96.2</b>

TABLE V  
ABLATION RESULTS FOR FEW-SHOT BRANCH. *PM* STANDS FOR ORIGINAL PATCH MATCHING, *GDINO* FOR GROUNDING DINO, AND *VL* FOR VISION-LANGUAGE FEATURE MATCHING. *Img-AUC* AND *Px-AUC* REPRESENT IMAGE-LEVEL AND PIXEL-LEVEL AUC, RESPECTIVELY. THE BEST-PERFORMING METHOD IS IN BOLD.

Setup	Method	MVTec-AD		VisA	
		Img-AUC	Px-AUC	Img-AUC	Px-AUC
1-shot	PM	94.9	94.8	80.6	<b>97.3</b>
	+ GDINO	<b>95.0</b>	<b>96.2</b>	81.7	<b>97.3</b>
	+ VL	<b>95.0</b>	<b>96.2</b>	<b>88.3</b>	<b>97.3</b>
2-shot	PM	<b>95.8</b>	95.3	80.8	<b>97.5</b>
	+ GDINO	<b>95.8</b>	96.5	82.0	<b>97.5</b>
	+ VL	<b>95.8</b>	<b>96.5</b>	<b>88.6</b>	<b>97.5</b>
4-shot	PM	<b>96.3</b>	95.6	85.6	<b>97.9</b>
	+ GDINO	<b>96.3</b>	96.6	87.3	<b>97.9</b>
	+ VL	<b>96.3</b>	<b>96.6</b>	<b>89.8</b>	<b>97.9</b>

TABLE VI  
COMPARISON OF DIFFERENT LEARNING METHODS FOR LEARNABLE VECTORS AND WHETHER TO USE CLASS NAME. *Img-AUC* AND *Px-AUC* REPRESENT IMAGE-LEVEL AND PIXEL-LEVEL AUC, RESPECTIVELY. THE BEST-PERFORMING METHOD IS IN BOLD.

Learning method	CLS name	MVTec-AD		VisA	
		Img-AUC	Px-AUC	Img-AUC	Px-AUC
CoOp		90.1	88.8	82.0	95.5
CoOp	✓	89.9	90.4	81.2	95.4
CoCoOp		91.5	90.8	82.7	95.7
<b>CoCoOp</b>	✓	<b>92.1</b>	<b>92.8</b>	<b>84.5</b>	<b>96.2</b>

mance against several state-of-the-art few-shot anomaly detection methods, including SPADE [45], PatchCore [10], WinCLIP [13], and AnomalyGPT [43]. In this setting, unlike the zero-shot scenario, a small number of normal samples from the test classes are provided for reference during testing. We conducted experiments under 1-shot, 2-shot, and 4-shot configurations respectively.

Table II presents a performance comparison between our FiLo++ and other few-shot anomaly detection methods. The results reveal that FiLo++ achieves a marked performance improvement over conventional patch-matching approaches under few-shot settings, particularly in the 1-shot scenario. This highlights the effectiveness of FiLo++’s vision-language matching and position-enhanced patch matching approach in few-shot anomaly detection.

TABLE VII  
COMPARISON OF DIFFERENT LLMs USED TO GENERATE ANOMALY DESCRIPTIONS. THE BEST-PERFORMING METHOD IS IN BOLD.

LLM	VisA		MVTec-AD	
	Image-AUC	Pixel-AUC	Image-AUC	Pixel-AUC
<b>GPT-4o</b>	<b>84.5</b>	<b>96.2</b>	<b>92.1</b>	<b>92.8</b>
GPT-3.5	84.3	96.2	91.8	92.6
Llama	84.4	96.0	91.9	92.5

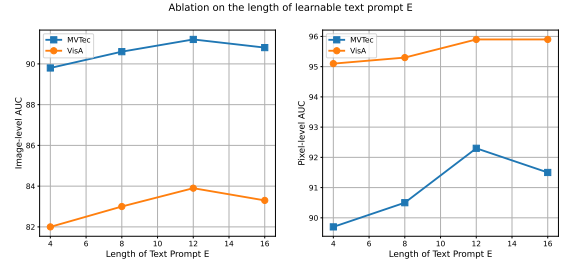


Fig. 3. Comparison of FiLo++ on MVTec and VisA datasets with different numbers of learnable vectors.

F. Ablation Study

In order to validate the effectiveness of each proposed module, we conducted extensive ablation experiments on the MVTec AD and VisA datasets. These experiments examined various components in both FusDes and DefLoc, the usage of vision-language features and location enhancement in few-shot anomaly detection, the implementation strategies for learnable text vectors, the application of V-V Attention, and the impact of different convolutional kernels in the MDCI module.

In Table III, we begin with the baseline model CLIP-AC, utilizing simple two-category texts “A photo of a normal

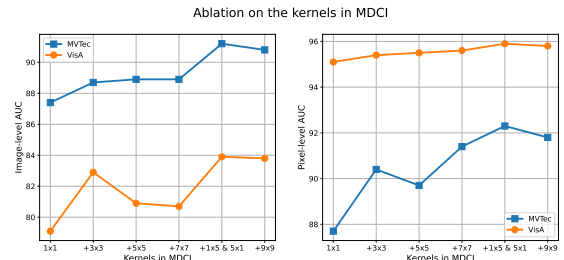


Fig. 4. Comparison of FiLo++ on MVTec and VisA datasets with different convolution kernels.



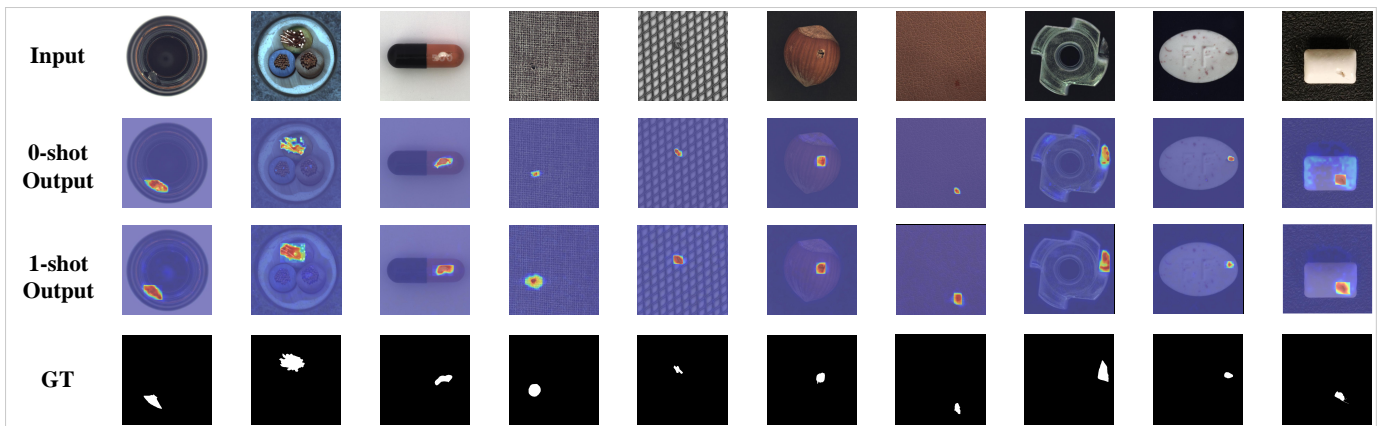


Fig. 5. 0-shot and 1-shot visualization results of FiLo++ on the MVTec-AD and VisA datasets. It can be observed that FiLo++ achieves anomaly segmentation results that closely approximate the ground truth even when only language or a very limited number of normal samples are provided as references.

[class]” and “A photo of an anomalous [class]”. Building upon this foundation, we progressively incorporate generic state descriptions, fine-grained anomaly descriptions generated by large language models, learnable prompt templates, and runtime prompt filtering strategies. The experimental results demonstrate that more detailed and customized textual descriptions significantly enhance the performance of anomaly detection methods based on vision-language feature matching.

In Table IV, we further conduct ablation experiments on the modules within DefLoc. Both Grounding DINO and Position Enhancement contribute to the improvement of pixel-level AUC. Additionally, the MDCI module integrates multi-scale and deformable functionalities, effectively detecting anomalies of various sizes and shapes, thereby enhancing both detection and localization performance.

Subsequently, in Table V, we assess the performance impact of Grounding DINO and vision-language feature comparison within FiLo++ on few-shot anomaly detection. The results indicate that both components of FiLo++ provide performance enhancements to the original patch-matching-based few-shot anomaly detection methods.

In Table VI and Figure 3, we experiment with different parameters of the learnable text vectors, including the number of learnable vectors, the choice between CoOp [17] and CoCoOp [46] for the learning method, and whether to include the object class names in the prompts. The experiments reveal that the optimal performance is achieved when the number of learnable vectors is set to 12. Furthermore, the results show that when using CoOp, omitting the class names from the text leads to better performance, consistent with findings in AnomalyCLIP. This is because CoOp inherently emphasizes the generality and uniformity of text prompts. In contrast, when using CoCoOp to learn text templates, including class name information enhances performance. This improvement is attributed to CoCoOp’s approach of integrating image features into text prompts through a meta-network, which aligns with FiLo++’s use of fine-grained anomaly descriptions and position enhancement to obtain precise representations of each image’s content, thereby better matching the image content.

In Table VII, we compare the model’s performance when

generating detailed anomaly descriptions using different large language models. The experimental results demonstrate that employing various LLMs to produce detailed anomaly descriptions has only a minor impact on the outcomes.

In Figure 4, we also compare the impact of different sizes and shapes of modules within MDCI on the final performance, thereby validating the effectiveness of our multi-scale and multi-shape approach.

### G. Visualization Results

Fig 5 illustrates the 0-shot and 1-shot visualization results of FiLo++ on the MVTec-AD and VisA datasets, demonstrating FiLo++’s robust anomaly localization capability.

## V. CONCLUSION

In this paper, we propose FiLo++, a zero-shot and few-shot anomaly detection framework that addresses the dual challenges of precise detection and accurate localization. By leveraging the FusDes module, which combines the knowledge of large language models with both fixed and learnable text prompts, FiLo++ effectively adapts to diverse anomaly types. The DefLoc module further refines localization through Grounding DINO, position-enhanced text descriptions, and a multi-scale deformable cross-modal interaction module to better handle anomalies of varying shapes and sizes. Additionally, a position-enhanced patch matching strategy boosts few-shot performance by focusing on suspicious regions during inference. Extensive experimental results on MVTec-AD and VisA datasets demonstrate that FiLo++ outperforms existing approaches in both zero-shot and few-shot scenarios, highlighting the potential of integrating powerful language models with advanced vision techniques for anomaly detection.

## REFERENCES

- [1] B. Zhu, Z. Gu, G. Zhu, Y. Chen, M. Tang, and J. Wang, “Adformer: Generalizable few-shot anomaly detection with dual cnn-transformer architecture,” *IEEE Transactions on Instrumentation and Measurement*, 2024.
- [2] Y. Jiang, X. Lu, Q. Jin, Q. Sun, H. Wu, and C. Zhuo, “Fabgpt: An efficient large multimodal model for complex wafer defect knowledge queries,” *arXiv preprint arXiv:2407.10810*, 2024.

- [3] B. Zhu, Y. Chen, M. Tang, and J. Wang, "Pixel-level contrastive pre-trainer for industrial image representation," *IEEE Transactions on Instrumentation and Measurement*, 2024.
- [4] C. Huang, Q. Xu, Y. Wang, Y. Wang, and Y. Zhang, "Self-supervised masking for unsupervised anomaly detection and localization," *IEEE Transactions on Multimedia*, vol. 25, pp. 4426–4438, 2022.
- [5] J. Bao, H. Sun, H. Deng, Y. He, Z. Zhang, and X. Li, "Bmad: Benchmarks for medical anomaly detection," in *Proceedings of the IEEE/CVF Conference on Computer Vision and Pattern Recognition*, 2024, pp. 4042–4053.
- [6] C. Huang, A. Jiang, J. Feng, Y. Zhang, X. Wang, and Y. Wang, "Adapting visual-language models for generalizable anomaly detection in medical images," in *Proceedings of the IEEE/CVF Conference on Computer Vision and Pattern Recognition*, 2024, pp. 11 375–11 385.
- [7] H. Shi, L. Wang, S. Zhou, G. Hua, and W. Tang, "Abnormal ratios guided multi-phase self-training for weakly-supervised video anomaly detection," *IEEE Transactions on Multimedia*, 2023.
- [8] S. Chang, Y. Li, S. Shen, J. Feng, and Z. Zhou, "Contrastive attention for video anomaly detection," *IEEE Transactions on Multimedia*, vol. 24, pp. 4067–4076, 2021.
- [9] N. Li, F. Chang, and C. Liu, "Spatial-temporal cascade autoencoder for video anomaly detection in crowded scenes," *IEEE Transactions on Multimedia*, vol. 23, pp. 203–215, 2020.
- [10] K. Roth, L. Pemula, J. Zepeda, B. Schölkopf, T. Brox, and P. Gehler, "Towards total recall in industrial anomaly detection," in *Proceedings of the IEEE/CVF conference on computer vision and pattern recognition*, 2022, pp. 14 318–14 328.
- [11] T. Defard, A. Setkov, A. Loesch, and R. Audigier, "Padim: a patch distribution modeling framework for anomaly detection and localization," in *International Conference on Pattern Recognition*. Springer, 2021, pp. 475–489.
- [12] Z. You, L. Cui, Y. Shen, K. Yang, X. Lu, Y. Zheng, and X. Le, "A unified model for multi-class anomaly detection," *Advances in Neural Information Processing Systems*, vol. 35, pp. 4571–4584, 2022.
- [13] J. Jeong, Y. Zou, T. Kim, D. Zhang, A. Ravichandran, and O. Dabeer, "Winclip: Zero-/few-shot anomaly classification and segmentation," in *Proceedings of the IEEE/CVF Conference on Computer Vision and Pattern Recognition*, 2023, pp. 19 606–19 616.
- [14] C. Huang, H. Guan, A. Jiang, Y. Zhang, M. Spratling, and Y.-F. Wang, "Registration based few-shot anomaly detection," in *European Conference on Computer Vision*. Springer, 2022, pp. 303–319.
- [15] Z. Gu, B. Zhu, G. Zhu, Y. Chen, H. Li, M. Tang, and J. Wang, "Filo: Zero-shot anomaly detection by fine-grained description and high-quality localization," in *Proceedings of the 32nd ACM International Conference on Multimedia*, 2024, pp. 2041–2049.
- [16] A. Radford, J. W. Kim, C. Hallacy, A. Ramesh, G. Goh, S. Agarwal, G. Sastry, A. Askell, P. Mishkin, J. Clark *et al.*, "Learning transferable visual models from natural language supervision," in *International conference on machine learning*. PMLR, 2021, pp. 8748–8763.
- [17] K. Zhou, J. Yang, C. C. Loy, and Z. Liu, "Learning to prompt for vision-language models," *International Journal of Computer Vision*, vol. 130, no. 9, pp. 2337–2348, 2022.
- [18] S. Chen, F. Meng, R. Zhang, H. Qiu, H. Li, Q. Wu, and L. Xu, "Visual and textual prior guided mask assemble for few-shot segmentation and beyond," *IEEE Transactions on Multimedia*, 2024.
- [19] H. Shi, H. Li, Q. Wu, and K. N. Ngan, "Query reconstruction network for referring expression image segmentation," *IEEE Transactions on Multimedia*, vol. 23, pp. 995–1007, 2020.
- [20] S. Liu, Z. Zeng, T. Ren, F. Li, H. Zhang, J. Yang, Q. Jiang, C. Li, J. Yang, H. Su *et al.*, "Grounding dino: Marrying dino with grounded pre-training for open-set object detection," in *European Conference on Computer Vision*. Springer, 2025, pp. 38–55.
- [21] J. Deng, W. Dong, R. Socher, L.-J. Li, K. Li, and L. Fei-Fei, "Imagenet: A large-scale hierarchical image database," in *2009 IEEE conference on computer vision and pattern recognition*. Ieee, 2009, pp. 248–255.
- [22] X. Zhu, H. Hu, S. Lin, and J. Dai, "Deformable convnets v2: More deformable, better results," in *Proceedings of the IEEE/CVF conference on computer vision and pattern recognition*, 2019, pp. 9308–9316.
- [23] P. Bergmann, M. Fauser, D. Sattlegger, and C. Steger, "Mvtec ad—a comprehensive real-world dataset for unsupervised anomaly detection," in *Proceedings of the IEEE/CVF conference on computer vision and pattern recognition*, 2019, pp. 9592–9600.
- [24] Y. Zou, J. Jeong, L. Pemula, D. Zhang, and O. Dabeer, "Spot-the-difference self-supervised pre-training for anomaly detection and segmentation," in *European Conference on Computer Vision*. Springer, 2022, pp. 392–408.
- [25] P. Liznerski, L. Ruff, R. A. Vandermeulen, B. J. Franks, K.-R. Müller, and M. Kloft, "Exposing outlier exposure: What can be learned from few, one, and zero outlier images?" *arXiv preprint arXiv:2205.11474*, 2022.
- [26] S. Esmailpour, B. Liu, E. Robertson, and L. Shu, "Zero-shot out-of-distribution detection based on the pre-trained model clip," in *Proceedings of the AAAI conference on artificial intelligence*, vol. 36, no. 6, 2022, pp. 6568–6576.
- [27] X. Chen, Y. Han, and J. Zhang, "April-gan: A zero-/few-shot anomaly classification and segmentation method for cvpr 2023 vand workshop challenge tracks 1&2: 1st place on zero-shot ad and 4th place on few-shot ad," *arXiv preprint arXiv:2305.17382*, 2023.
- [28] Y. Li, H. Wang, Y. Duan, and X. Li, "Clip surgery for better explainability with enhancement in open-vocabulary tasks," *arXiv preprint arXiv:2304.05653*, 2023.
- [29] H. Deng, Z. Zhang, J. Bao, and X. Li, "Anovl: Adapting vision-language models for unified zero-shot anomaly localization," *arXiv preprint arXiv:2308.15939*, 2023.
- [30] Q. Zhou, G. Pang, Y. Tian, S. He, and J. Chen, "Anomalyclip: Object-agnostic prompt learning for zero-shot anomaly detection," *arXiv preprint arXiv:2310.18961*, 2023.
- [31] Y. Cao, X. Xu, C. Sun, Y. Cheng, Z. Du, L. Gao, and W. Shen, "Segment any anomaly without training via hybrid prompt regularization," *arXiv preprint arXiv:2305.10724*, 2023.
- [32] A. Kirillov, E. Mintun, N. Ravi, H. Mao, C. Rolland, L. Gustafson, T. Xiao, S. Whitehead, A. C. Berg, W.-Y. Lo *et al.*, "Segment anything," in *Proceedings of the IEEE/CVF International Conference on Computer Vision*, 2023, pp. 4015–4026.
- [33] M. Jaderberg, K. Simonyan, A. Zisserman *et al.*, "Spatial transformer networks," *Advances in neural information processing systems*, vol. 28, 2015.
- [34] J. Liao, X. Xu, M. C. Nguyen, A. Goodge, and C. S. Foo, "Coft-ad: Contrastive fine-tuning for few-shot anomaly detection," *IEEE Transactions on Image Processing*, 2024.
- [35] C. Szegedy, W. Liu, Y. Jia, P. Sermanet, S. Reed, D. Anguelov, D. Erhan, V. Vanhoucke, and A. Rabinovich, "Going deeper with convolutions," in *Proceedings of the IEEE conference on computer vision and pattern recognition*, 2015, pp. 1–9.
- [36] X. Ding, X. Zhang, N. Ma, J. Han, G. Ding, and J. Sun, "Repvgg: Making vgg-style convnets great again," in *Proceedings of the IEEE/CVF conference on computer vision and pattern recognition*, 2021, pp. 13 733–13 742.
- [37] M. Tan and Q. V. Le, "Mixconv: Mixed depthwise convolutional kernels," *arXiv preprint arXiv:1907.09595*, 2019.
- [38] J. Zhu, S. Cai, F. Deng, B. C. Ooi, and J. Wu, "Do llms understand visual anomalies? uncovering llm's capabilities in zero-shot anomaly detection," in *Proceedings of the 32nd ACM International Conference on Multimedia*, 2024, pp. 48–57.
- [39] X. Glorot, A. Bordes, and Y. Bengio, "Deep sparse rectifier neural networks," in *Proceedings of the fourteenth international conference on artificial intelligence and statistics*. JMLR Workshop and Conference Proceedings, 2011, pp. 315–323.
- [40] S. Elfving, E. Uchibe, and K. Doya, "Sigmoid-weighted linear units for neural network function approximation in reinforcement learning," *Neural networks*, vol. 107, pp. 3–11, 2018.
- [41] T.-Y. Lin, P. Goyal, R. Girshick, K. He, and P. Dollár, "Focal loss for dense object detection," in *Proceedings of the IEEE international conference on computer vision*, 2017, pp. 2980–2988.
- [42] F. Milletari, N. Navab, and S.-A. Ahmadi, "V-net: Fully convolutional neural networks for volumetric medical image segmentation," in *2016 fourth international conference on 3D vision (3DV)*. Ieee, 2016, pp. 565–571.
- [43] Z. Gu, B. Zhu, G. Zhu, Y. Chen, M. Tang, and J. Wang, "Anomalygpt: Detecting industrial anomalies using large vision-language models," in *Proceedings of the AAAI Conference on Artificial Intelligence*, vol. 38, no. 3, 2024, pp. 1932–1940.
- [44] I. Loshchilov and F. Hutter, "Decoupled weight decay regularization," *arXiv preprint arXiv:1711.05101*, 2017.
- [45] N. Cohen and Y. Hoshen, "Sub-image anomaly detection with deep pyramid correspondences," *arXiv preprint arXiv:2005.02357*, 2020.
- [46] K. Zhou, J. Yang, C. C. Loy, and Z. Liu, "Conditional prompt learning for vision-language models," in *Proceedings of the IEEE/CVF conference on computer vision and pattern recognition*, 2022, pp. 16 816–16 825.